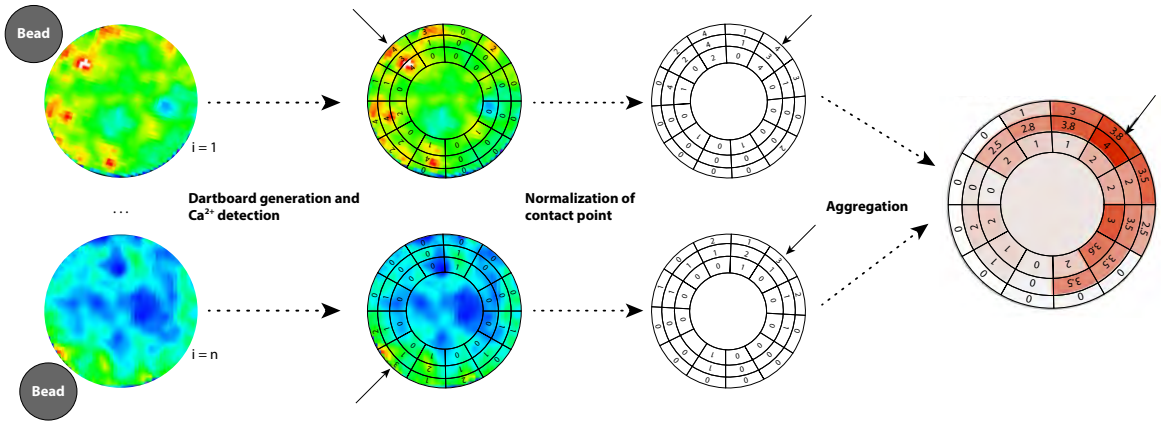

Fig. S1 Generation of dartboard projection

Dartboard workflow: First a dartboard is projected on every T cell (i=1 to n). Then, all T cells are spatio-temporally normalized for bead contact site and time. The mean number of Ca^{2+} microdomains is analyzed and depicted as dartboard; data are available for the whole cell, each dartboard sections, or combinations of such sections. Sections (or combinations) can be selected for further subcellular analysis.

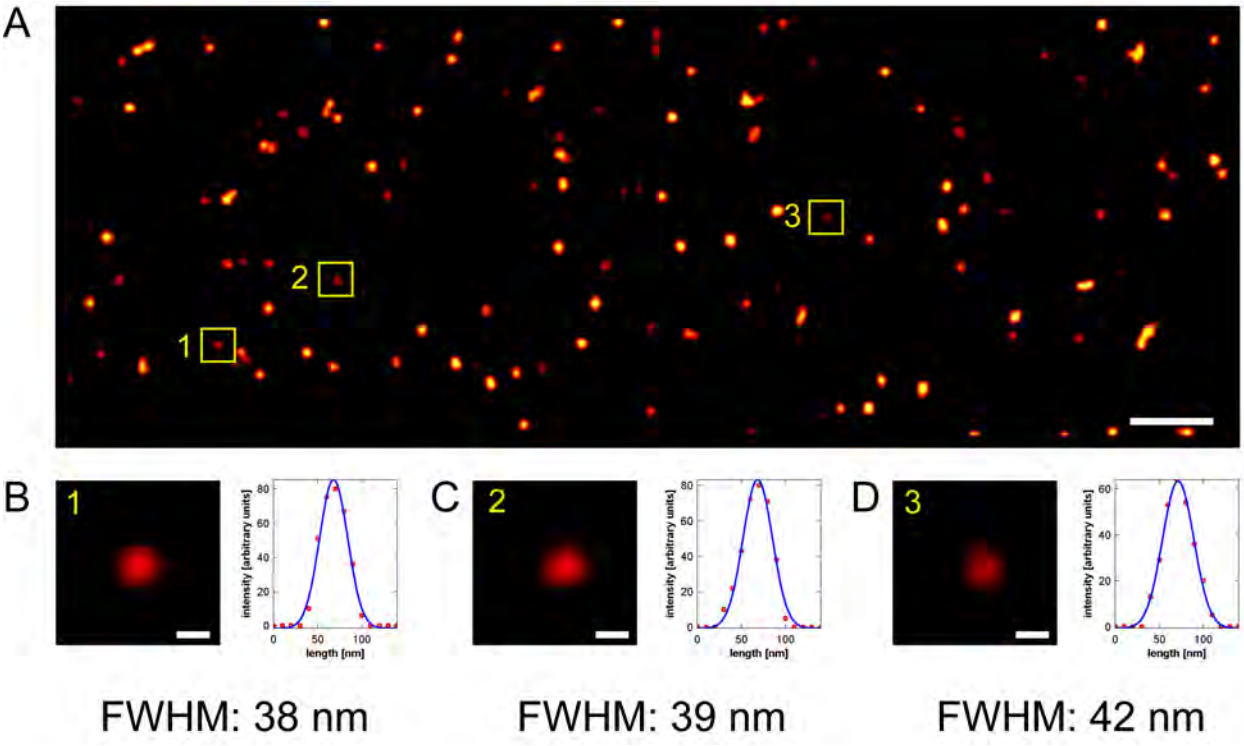

Fig. S2 Resolution of the STED microscope

40 nm Crimson beads were scanned in STED mode to estimate the system resolution. From a large field of view (A), 10 individual beads were selected to determine the FWHM, 3 of which are shown in (B-D) along with the Gaussian-fit function. Scale bars: (A) 500 nm, (B-D): 40 nm. In this way, a FWHM of 41 ± 3nm (n=10) for the individual Crimson bead was measured. Thus the STED microscope, in the configuration it was used during the experiment described can resolve nano-objects up to 40 nm apart from each other.

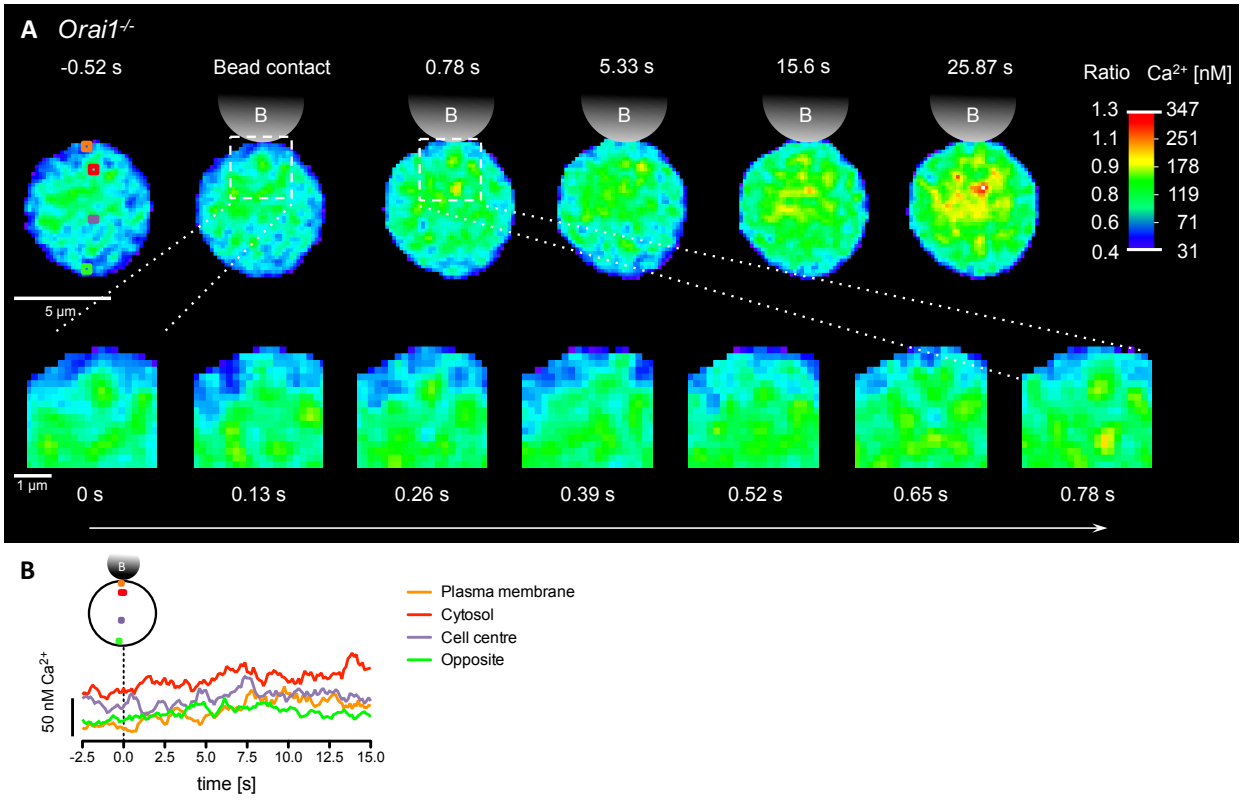

Fig. S3 Example of an *Orai1*$^{-/-}$ T cell with Ca^{2+} microdomains occurring more deeply within the cytosol

(A) Initial Ca^{2+} microdomains in an representative *Orai1*$^{-/-}$ T cell (total number of *Orai1*$^{-/-}$ T cells analyzed = 28) with Ca^{2+} microdomains occurring more deeply within the cytosol upon anti-CD3/anti-CD28 stimulation (bead contact; indicated schematically) and a magnified region near the bead contact. (B) Respective Ca^{2+} tracings of four ROIs (3x3 pixel) shown in (A). Dashed line indicates time point of bead contact.

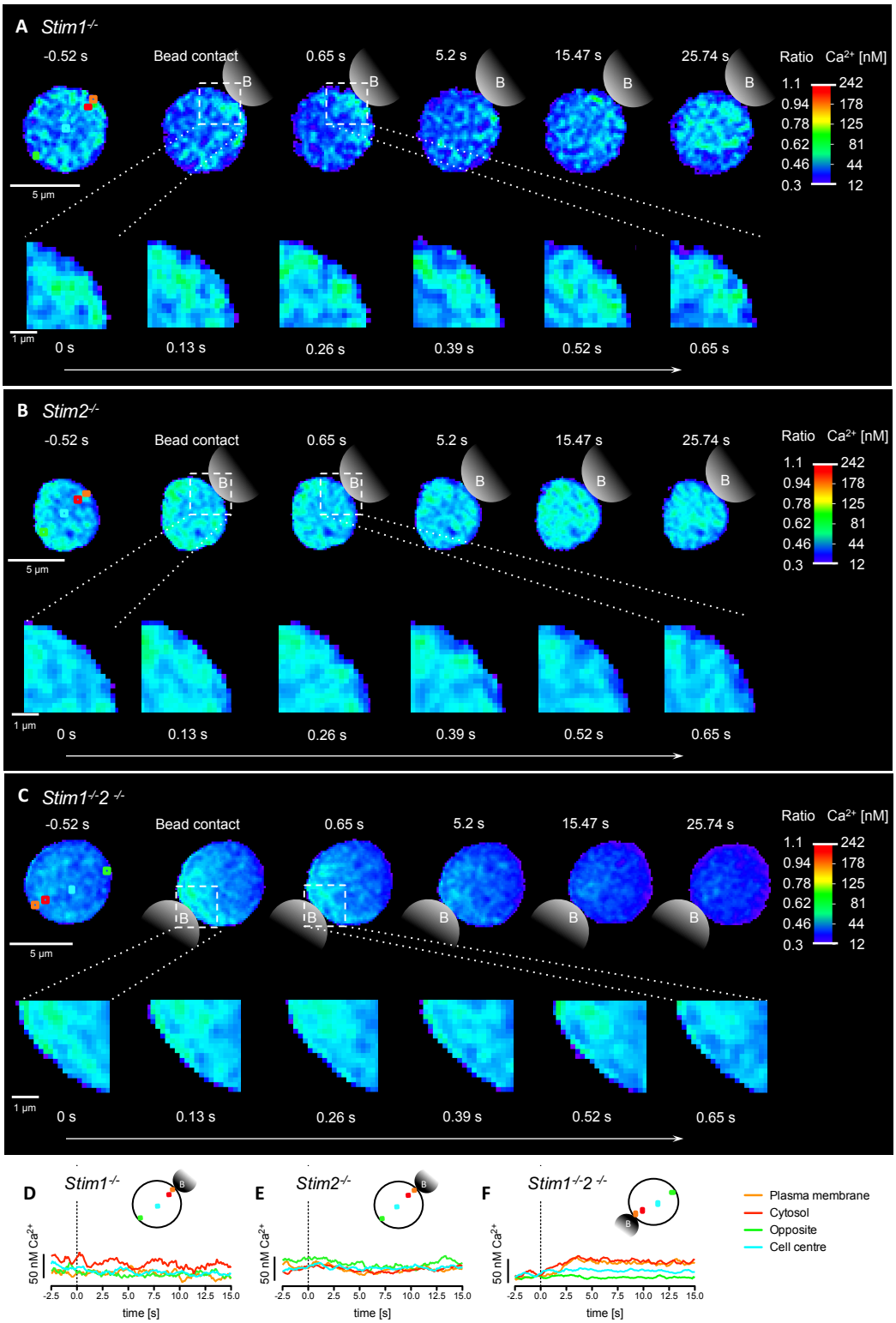

Fig. S4 Markedly decreased initial Ca^{2+} microdomains in *Stim1*$^{-/-}$, *Stim2*$^{-/-}$ and *Stim1*$^{-/-}$/*2*$^{-/-}$ T cells

Initial Ca^{2+} microdomains in representative cells, a *Stim1*$^{-/-}$ T cell (A; total number of *Stim1*$^{-/-}$ T cell analyzed =24), a CD4+ *Stim2*$^{-/-}$ T cell (B; total number of *Stim2*$^{-/-}$ T cells analyzed =39) and a *Stim1*$^{-/-}$/*2*$^{-/-}$ (C; total number of *Stim1*$^{-/-}$/*2*$^{-/-}$ T cells analyzed =46) upon bead contact (indicated schematically) and a magnified region near the bead contact. (D-F) Respective Ca^{2+} tracings of the four ROIs (3x3 pixel) shown in (A-C, as indicated). Dashed lines indicate the time point of bead contact.

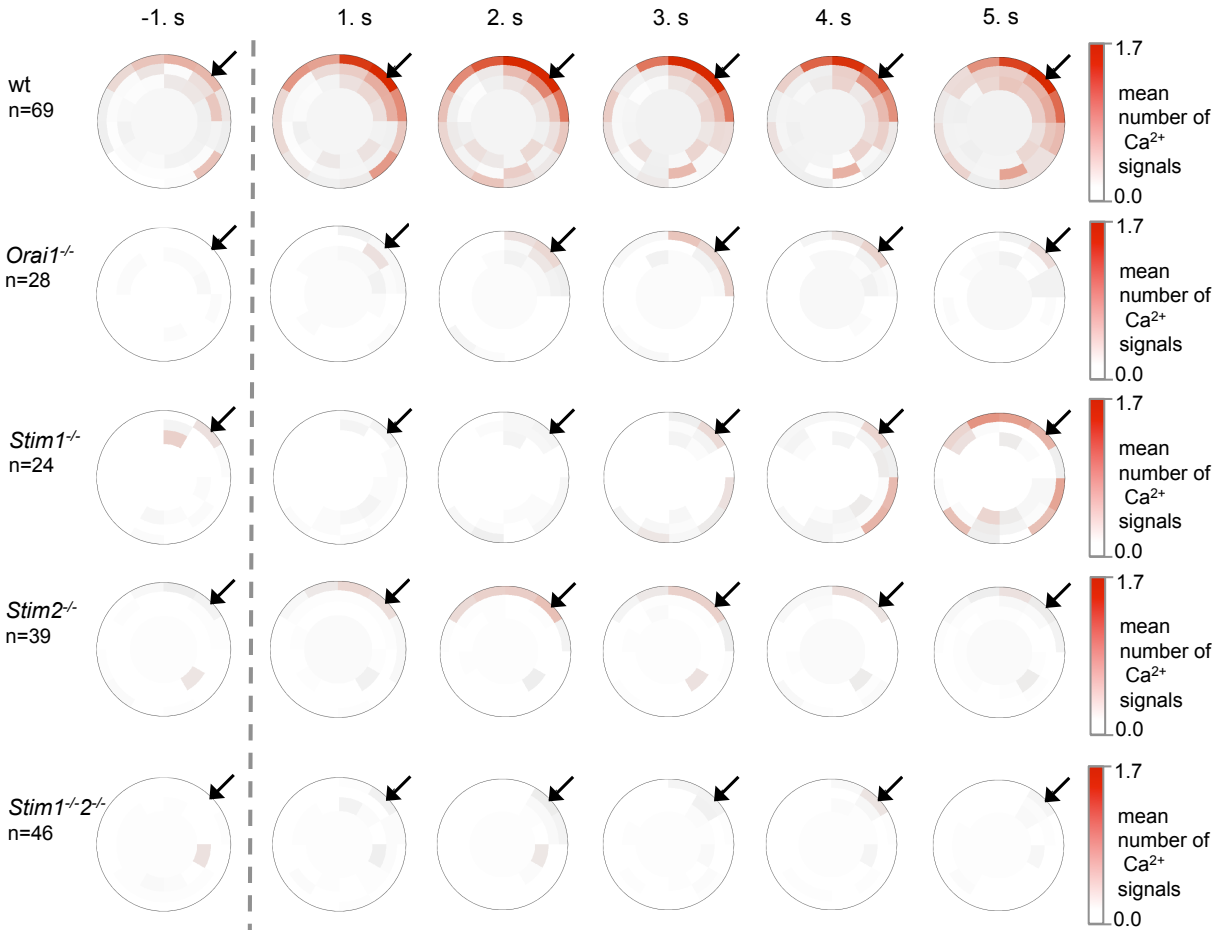

Fig. S5 Comparison of initial Ca^{2+} microdomains in primary murine T cells in a dartboard projection

Primary wt (n = 69 cells), *Orai1*$^{-/-}$ (n = 28 cells), *Stim1*$^{-/-}$ (n = 24 cells), *Stim2*$^{-/-}$ (n = 39 cells), *Stim1*$^{-/-}$*2*$^{-/-}$ (n = 46 cells) were stimulated by anti-CD3/anti-CD28 coated beads; the bead contact site is indicated as black arrow. Initial Ca^{2+} signals as detected in the last second before stimulation (-1.sec), or in the 1st second (1. sec) until 5th second (5. sec).
T cells were normalized spatially regarding the bead contact site and the time of bead contact. The dartboard shows mean values of number of Ca^{2+} signals in all T cells (for each genotype as indicated). Max. relative value is 1.7 (dark red) as indicated.

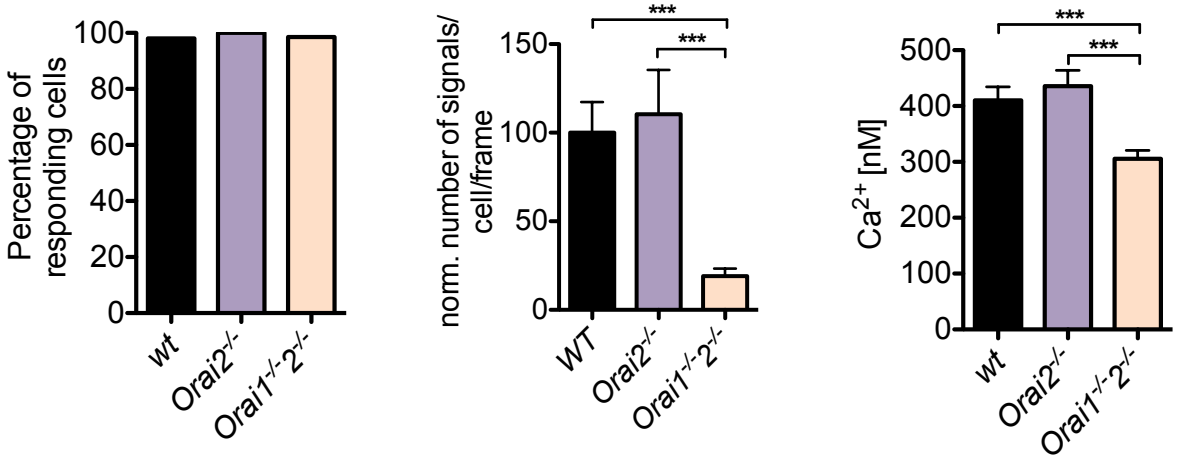

Fig. S6 *Orai2*$^{-/-}$ is not involved in the formation of initial Ca^{2+} microdomains
Characteristics of initial Ca^{2+} microdomains in primary murine CD4+ wt (n=28), *Orai2*$^{-/-}$ (n=20) and Orai*1*$^{-/-}$*2*$^{-/-}$ (n=35) in the first 15 sec following bead contact. Comparison of the percentage of responding cells, the number of signals per cell and frame and the Ca^{2+} amplitude (data represent mean ± SEM). Statistically significant differences are marked by asterisks (* $p<0.05$, ** $p<0.01$, *** $p<0.001$, Kruskal-Wallis Test).

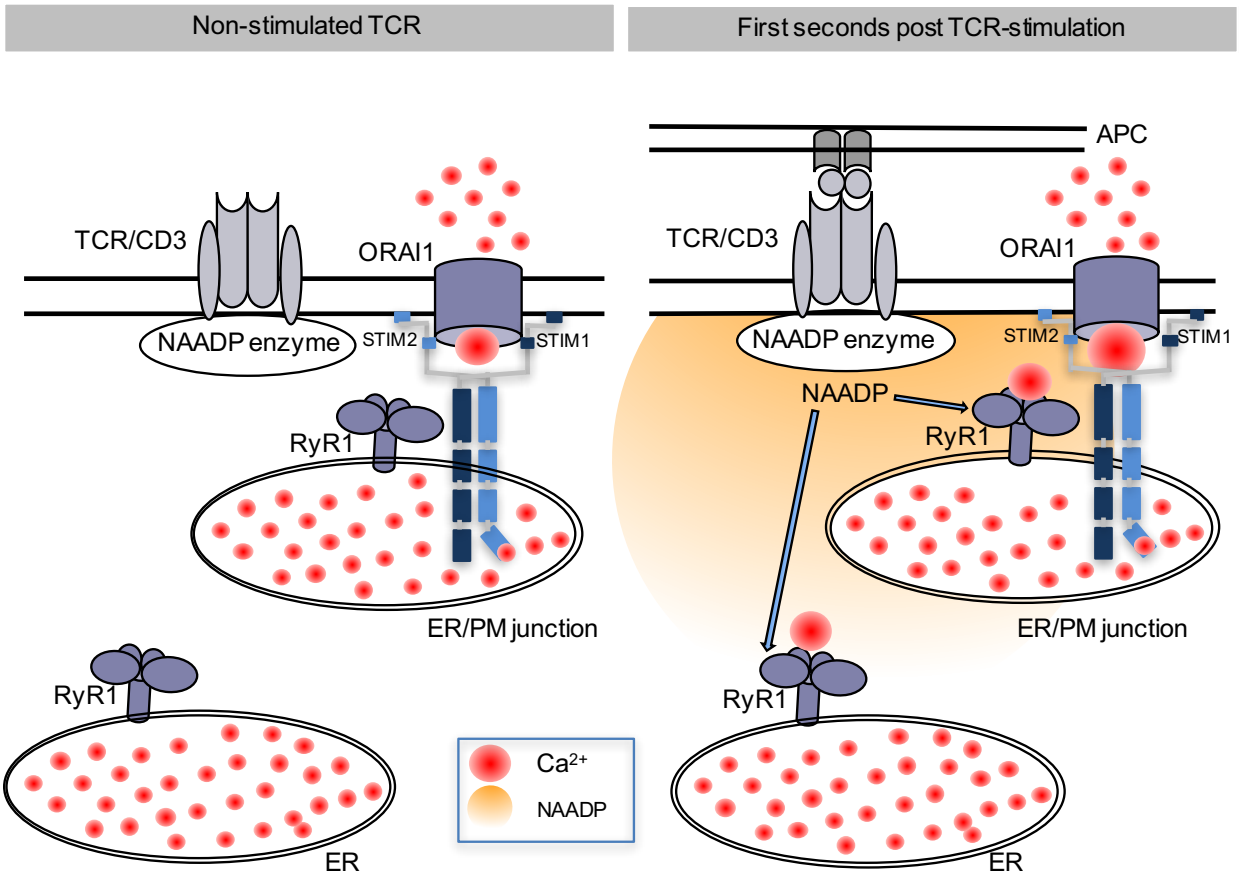

Fig. S7 New model for the formation of initial Ca^{2+} microdomains in T cells

In non-stimulated T cells, ORAI1 and STIM1/STIM2 form protein complexes at defined plasma membrane sites resulting in spontaneous, discrete, local Ca^{2+} entry signals. These constitutive Ca^{2+} microdomains do not further propagate without cell activation. Upon TCR stimulation, RyR1 is activated, probably by NAADP formed within seconds of T cell stimulation, resulting in local and transient Ca^{2+} release. NAADP is believed to act via a binding protein, shown here tentatively as 'BP'. NAADP evoked Ca^{2+} release via RyR1 contributes directly to Ca^{2+} microdomains and, in addition, promotes the activation of STIM1, STIM2 and thus SOCE through ORAI1 channels thereby amplifying initial Ca^{2+} microdomains upon TCR stimulation. STIM1 and STIM2 are drawn here as heterodimers, as in (*28*); however, from our end there is no definitive experimental proof for such heterodimers.

Movie S1 Initial Ca^{2+} microdomains in a wt T cell after stimulation

Initial Ca^{2+} microdomains in a wt T cell upon bead contact (indicated schematically at timepoint = 0). Acquisition speed was 40 frames/s, movie playback at 20 frames/s. Length scale bar and ratio as indicated. Five subsequent images were merged to decrease noise.

Movie S2 *Orai1*$^{-/-}$ T cell upon bead contact

Decreased initial Ca^{2+} microdomains in a representative *Orai1*$^{-/-}$ T cell upon bead contact (indicated schematically at timepoint = 0). Acquisition speed was 40 frames/s, movie playback at 20 frames/s. Length scale bar and ratio as indicated. Five subsequent images were merged to decrease noise.

Movie S3 *Stim1*$^{-/-}$*2*$^{-/-}$ T cell upon bead contact

Decreased initial Ca^{2+} microdomains in a representative *Stim1*$^{-/-}$*2*$^{-/-}$ T cell upon bead contact (indicated schematically at timepoint = 0). Acquisition speed was 40 frames/s, movie playback at 20 frames/s. Length scale bar and ratio as indicated. Five subsequent images were merged to decrease noise.